QUARTERLY JOURNAL OF THE ROYAL METEOROLOGICAL SOCIETY
Q. J. R. Meteorol. Soc. **135**: 1230–1247 (2009)
Published online 10 July 2009 in Wiley InterScience
(www.interscience.wiley.com) DOI: 10.1002/qj.434

On the theory relating changes in area-average and pan evaporation

W. James Shuttleworth,[a,b]* Aleix Serrat-Capdevila,[a] Michael L. Roderick[c] and Russell L. Scott[d]

[a]*SAHRA, Department of Hydrology and Water Resources, University of Arizona, Tucson, Arizona, USA*
[b]*Joint Centre for Hydrometeorological Research, Center for Ecology and Hydrology, Wallingford, UK*
[c]*Research Schools of Biological and Earth Sciences, The Australian National University, Canberra, Australia*
[d]*Southwest Watershed Research Center, USDA-ARS, Tucson, Arizona, USA*

ABSTRACT: Theory relating changes in area-average evaporation with changes in the evaporation from pans or open water is developed. Such changes can arise by Type (a) processes related to large-scale changes in atmospheric concentrations and circulation that modify surface evaporation rates in the same direction, and Type (b) processes related to coupling between the surface and atmospheric boundary layer (ABL) at the landscape scale that usually modify area-average evaporation and pan evaporation in different directions. The interrelationship between evaporation rates in response to Type (a) changes is derived. They have the same sign and broadly similar magnitude but the change in area-average evaporation is modified by surface resistance. As an alternative to assuming the complementary evaporation hypothesis, the results of previous modelling studies that investigated surface–atmosphere coupling are parametrized and used to develop a theoretical description of Type (b) coupling via vapour pressure deficit (VPD) in the ABL. The interrelationship between appropriately normalized pan and area-average evaporation rates is shown to vary with temperature and wind speed but, on average, the Type (b) changes are approximately equal and opposite. Long-term Australian pan evaporation data are analyzed to demonstrate the simultaneous presence of Type (a) and (b) processes, and observations from three field sites in southwestern USA show support for the theory describing Type (b) coupling via VPD.

KEY WORDS climate change; global dimming; complementary evaporation; evaporation paradox

Received 10 May 2008; Revised 23 January 2009; Accepted 9 April 2009

1. Introduction

Actual evaporation can be directly measured either by integrating water vapour transferred into the atmosphere or from the liquid water loss from representative sample volumes of the soil – atmosphere interface (Gash and Shuttleworth, 2007; Shuttleworth, 2008). However, all available methods are either too recent and/or too inaccurate (Farahani *et al.*, 2007; Shuttleworth, 2008) for them to be used to diagnose long-term change in actual evaporation. Consequently, researchers have sought alternative means to investigate such change. Attempts have been made to diagnose evaporation change as the residual in area-average water balance (e.g. Gedney *et al.*, 2006), but most studies have investigated long-term trends in the measured rate of pan evaporation or calculated rates of evaporation given by estimation equations. Unfortunately, the resulting literature has become confused and generated much controversy (e.g. Peterson *et al.*, 1995; Brutsaert and Parlange, 1998; Ohmura and Wild, 2002; Roderick and Farquhar, 2002, 2004, 2005; Hobbins *et al.*, 2004; Brutsaert, 2006; Kahler and Brutsaert, 2006, Roderick *et al.*, 2007). In part, this is because most of these studies have been couched in terms of early evaporation theory, including the abstract concepts of *potential evaporation* and *potential evapotranspiration* and the hypothetical concept of *complementary evaporation* (CE; Bouchet, 1963). The present paper reconsiders the theory relating gradual change in area-average to pan evaporation on the basis of actual evaporation rates.

Evaporation is controlled by the availability of water accessible to the atmosphere and by diffusion processes that inhibit surface evaporation, but is also controlled by near-surface atmospheric variables. Long-term changes in the near-surface atmospheric variables that control evaporation can arise in two ways:

(a) Large- or regional-scale changes in the atmosphere as a whole that are then reflected in near-surface values;
(b) Landscape-scale changes in the near-surface climate that arise from altered feedback between the surface and the atmospheric boundary layer (ABL) in response to changes in surface controls on area-average evaporation.

Because atmospheric variables exert a broadly similar influence on all evaporation rates if surface controls

*Correspondence to: W. J. Shuttleworth, SAHRA, Dept. of Hydrology and Water Resources, University of Arizona, Tucson, AZ, USA.
E-mail: jshuttle@hwr.arizona.edu

are unaltered, Type (a) changes will tend to modify all evaporation rates in the same direction, and evaporation from the landscape and from any well-watered crop, open water, and evaporation pans within the landscape will all either increase or decrease. For Type (b) changes, surface variables alter because landscape-average surface controls alter. Higher area-average evaporation may, for example, decrease the vapour pressure deficit (VPD) or near-surface wind speed (by reducing turbulence) in the ABL, or may alter surface solar radiation by changing boundary-layer cloud cover. The resulting changes in atmospheric variables in the ABL will alter evaporation rates from portions of the landscape where surface controls remain unaltered, including from well-watered crops, open water, and evaporation pans.

A full description of changes in actual surface evaporation rates will ultimately require using models that simultaneously describe Type (a) and (b) changes. Pending the availability of such models, the present paper explores the theoretical relationships between changes in the evaporation rate from different evaporating surfaces for Type (a) and (b) changes separately, in the latter case with emphasis on exploring the adequacy or otherwise of representing surface – ABL coupling using the Bouchet (1963) CE hypothesis.

2. Actual evaporation rates

Reference crop evaporation (sometimes called *potential evapotranspiration*) is the actual evaporation rate from a well-watered, well-specified grass crop estimated from an implementation (Allen *et al.*, 1998) of the Penman–Monteith (P-M) equation (Monteith, 1965). *Open-water evaporation* (sometimes called *potential evaporation*) is the actual evaporation rate from stretches of open water and is frequently calculated from the Penman equation (Penman, 1948, 1963), this also being an implementation of the P-M equation. *Pan evaporation* is the actual measured evaporation from pans of water of differing design. In the past it has often been assumed to be related to open-water evaporation, adjusted downwards to allow for differences in surface energy availability using an empirical pan-specific correction factor, K_p. However, Rotstayn *et al.* (2006) have developed the 'PenPan' equation, a physically based description of pan evaporation based on the work of Thom *et al.* (1981) and Linacre (1994), which has been experimentally verified by Roderick *et al.* (2007) and which is also an implementation of the P-M equation. Finally, the actual area-average evaporation from the landscape can also be estimated from the P-M equation as described below.

The P-M equation (Monteith, 1965) calculates actual evaporation in the form of the latent heat flux, λE, from:

$$\lambda E = \frac{\Delta A + (\rho c_p D)/r_a}{\Delta + \gamma[1 + r_s/r_a]}, \tag{1}$$

where λ is the latent heat of vaporization of water; Δ is the rate of change of saturated vapour pressure with temperature; A is the energy available for evaporation at the evaporating surface, sometimes called the available energy; D is the VPD; γ is the psychrometric 'constant', ρ is the density of air and c_p is the specific heat of air at constant pressure. Different values or functions are selected for the surface resistance, r_s, and aerodynamic resistance, r_a, to calculate the evaporation rates of interest in the present study.

It is common practice when estimating crop water requirements (e.g. Allen *et al.*, 1998; Pereira *et al.*, 1999; Shuttleworth, 2006), to calculate the aerodynamic resistance between a vegetated surface and a level z_R using the equation:

$$r_a = \frac{\ln\left\{\frac{(z_R - d)}{z_0}\right\} . \ln\left\{\frac{(z_R - d)}{(z_0/10)}\right\}}{k^2 u_Z}, \tag{2}$$

where u_Z is the wind speed at the height z_R, $k = 0.41$ is the von Kármán constant, and d and z_0 are the zero-plane displacement and roughness length of the vegetated surface, respectively. Allen *et al.* (1998) specify the crop height, h_{rc}, for a reference crop as 0.12 m then set $z_0 = 0.123h_{rc}$, $d = 0.67h_{rc}$, and $r_s = 70$ s m^{-1}. In the present study, it is also assumed that it is acceptable to assume $z_0 = 0.123h_{aa}$ and $d = 0.67h_{aa}$ in Equation (2) when considering the area-average aerodynamic resistance for a landscape, with h_{aa} being the characteristic height of vegetation in the landscape. Later, it is shown that the results of the present analysis are little influenced by h_{aa} and it is arbitrarily set to 0.5 m, while the landscape average surface resistance is allowed to vary. For open-water evaporation, r_s is set to zero and $(r_a)_{ow} = 250/(1 + 0.536u_2)$ (Thom and Oliver, 1977). The PenPan equation implicitly assumes $(r_a)_{pan} = 224/(1 + 1.35u_2)$ and that the effective surface resistance of the pan is always 1.4 times the aerodynamic resistance.

The energy available to support evaporation differs depending on the evaporating surface. For simplicity in this study, energy storage terms are ignored and available energy is set equal to the net radiation, hence:

$$A = (1 - a)S + L_n, \tag{3}$$

where a is the albedo of the surface; S is the incoming solar radiation, and L_n is the net long-wave radiative exchange. Here the value of L_n is assumed independent of the surface and $a_{veg} = 0.23$ for both the area-average landscape and patches of reference crop within it, $a_{ow} = 0.08$ for open water surfaces and, following Rotstayn *et al.* (2006), $a_{pan} = 0.14$ for evaporation pans. Corresponding values of A are A_{veg}, A_{pan}, and A_{ow} for area-average and reference crop evaporation, evaporation pans, and open water, respectively. Table I summarizes the values and/or functions assumed for r_a, r_s, and a in the P-M equation when estimating the various evaporation rates.

DOI: 10.1002/qj

3. Specifying humid and arid conditions

Priestley and Taylor (1972) proposed the expression:

$$(\lambda E_{\mathrm{PT}})_{\alpha} = \alpha \frac{\Delta A}{\Delta + \gamma} \tag{4}$$

as an 'appropriate framework' for apportioning surface energy between sensible heat and evaporation, and reached 'the tentative conclusion that α is about 1.26 for saturated surfaces'. Equation (4) with α equal to 1.26 has sometimes been used to provide an alternative estimate of reference-crop evaporation, λE_{rc}, in humid conditions (Doorenbos and Pruitt, 1977; Shuttleworth, 1993). By equating reference crop evaporation rate to $(\lambda E_{\mathrm{PT}})_{\alpha}$, Shuttleworth (2006) specified the relationship between VPD at 2 m and available energy that define humid conditions in terms of the climatological resistance, r_{clim}, defined by the equation:

$$r_{\mathrm{clim}} = (\rho c_p D)/(\Delta A_{\mathrm{veg}}), \tag{5}$$

where A_{veg} is the available energy calculated with albedo equal to a_{veg}. (Note that climatological resistance has units of the other resistances in the P-M equation, but it is not a resistance that controls the rate of diffusion of energy fluxes.) With the aerodynamic and surface resistances for the reference crop given in Table I, equating λE_{rc} to $(\lambda E_{\mathrm{PT}})_{\alpha}$ gives:

$$r_{\mathrm{clim}} = \frac{208}{u_2}\left(\frac{\alpha[\Delta + \gamma(1 + 0.337u_2)]}{\Delta + \gamma} - 1\right). \tag{6}$$

Thus the value of r_{clim} in the humid conditions when $\lambda E_{\mathrm{rc}} = (\lambda E_{\mathrm{PT}})_{\alpha}$ with $\alpha = 1.26$, hereafter called $(\lambda E_{\mathrm{PT}})_{1.26}$, is a function of wind speed and temperature because Δ is a function of temperature. Jensen *et al.* (1990) propose $\alpha = 1.74$ as the value of α required for λE_{rc} to equal $(\lambda E_{\mathrm{PT}})_{\alpha}$ in arid conditions. When wind speed is 2 m s^{-1} and temperature 15°C, r_{clim} is 60 s m^{-1} and 123 s m^{-1} in humid and arid conditions, respectively.

4. Regional changes in actual evaporation rates

Large- or regional-scale Type (a) changes in the atmosphere as a whole influence all evaporation rates similarly. Some studies have investigated changes in the estimated rates of open-water and reference-crop evaporation using historical sunshine-hour data and calculated reductions in solar radiation of a few percent per decade (e.g. Chattopadhyay and Hume, 1997; Thomas, 2000; Chen *et al.*, 2005; Shenbin *et al.*, 2006; Xu *et al.*, 2006) implying either cloud cover or aerosol load, or both, have increased in some regions. Several studies (e.g. Askoy, 1997; Omran, 1998; Cohen *et al.*, 2002) have reported significant changes in observed solar radiation and confidently ascribed these to changes in atmospheric aerosol concentration, and the regionally varying but widespread impact of increasing atmospheric aerosols on surface solar radiation is documented in authoritative reviews (Ramanathan *et al.*, 2001; Stanhill and Cohen, 2001) and recognized and modelled in general circulation models (IPCC, 2007). Stanhill and Cohen (2001) estimated the reduction in solar radiation as 2.75% per decade while IPCC (2007) estimates the change in global radiative forcing due to sulphate aerosols since 1750 as between −0.2 and −0.8 W m^{-2}. Thus, there is strong evidence there has been a regionally dependent reduction in surface solar radiation, although this may now be decreasing (e.g. Wild *et al.*, 2005, 2007).

Most of the controversy regarding the origin of observed changes in pan evaporation has hitherto been concerned with the relative importance of reduced incoming solar radiation, on the one hand, and lower VPD caused by higher area-average evaporation, on the other. However, other causes exist. For example, recent studies of changes in pan evaporation in Australia have attributed most of the reduction in pan evaporation to reduced wind speed (Roderick *et al.*, 2007; Rayner, 2007; McVicar *et al.*, 2008). The cause of such a reduction in regional wind speed is not certain, although wind speed reductions have now been widely reported in midlatitudes in both hemispheres with roughly complementary increases in wind speed nearer the poles in general agreement with the predictions of climate models (Roderick *et al.*, 2007; McVicar *et al.*, 2008).

The relative changes in area-average evaporation, reference crop evaporation, open-water evaporation and pan evaporation rate (as estimated by the PenPan model) in response to small changes in meteorological variables due to large-scale processes can be estimated in the same way, because these different evaporation rates are all calculated by different implementations of Equation (1). In each case, a small change in evaporation rate is estimated

Table I. Functions and values to be substituted in Equations (1) and (3) to estimate the different actual evaporation rates considered in this paper, together with the associated expressions for the gradient of aerodynamic resistance with wind speed required in Equation (7).

Actual evaporation rate	Albedo, a	Surface resistance, r_s	Aerodynamic resistance, r_a	$(\partial r_a / \partial u_2)$
Area-average evaporation, λE_{aa}	0.23	(variable)	$110/u_2$	$-110/u_2^2$
Reference crop evaporation, λE_{rc}	0.23	70	$208/u_2$	$-208/u_2^2$
Open-water evaporation, λE_{ow}	0.08	0	$250/(1 + 0.536\ u_2)$	$-134/(1 + 0.536\ u_2)^2$
Pan evaporation (PenPan), λE_{pan}	0.14	$1.4\ r_a$	$224/(1 + 1.35\ u_2)$	$-302/(1 + 1.35\ u_2)^2$

DOI: 10.1002/qj

from the small changes in A, D, T, and u_2 by the expression:

$$\delta(\lambda E) = \left[\frac{\Delta r_a}{\Delta r_a + \gamma(r_a + r_s)}\right]\delta(A) + \left[\frac{\rho c_p}{\Delta r_a + \gamma(r_a + r_s)}\right]\delta(D) + \left[\gamma A \frac{(r_a + r_{clim})(r_a + r_s)}{[\Delta r_a + \gamma(r_a + r_s)]^2} \cdot \frac{\partial \Delta}{\partial T}\right]\delta(T) + \left[\Delta A \frac{\gamma r_s - (\Delta + \gamma) r_{clim}}{[\Delta r_a + \gamma(r_a + r_s)]^2} \cdot \frac{\partial r_a}{\partial u_2}\right]\delta(u_2). \quad (7)$$

In Equation (7) the value of r_{clim} is that calculated when the available energy relevant to the evaporating surface is substituted for A in Equation (5), i.e. A_{veg} for area-average evaporation and reference crop, and A_{pan} and A_{ow} for evaporation pans and open water, respectively. If changes in net long-wave radiation exchange, surface albedo and the energy stored in the soil and canopy are neglected, the change in available energy, δA, is estimated from δS, the change in incoming solar radiation, by:

$$\delta(A) = (1 - a)\delta(S). \quad (8)$$

Figure 1 shows fractional change in evaporation rates in response to small regional changes in available energy, VPD, temperature, and wind speed plotted as a function of the area-average surface resistance when the available energy is 200 W m^{-2}, temperature 15°C, the wind speed 2 m s^{-1} with the VPD corresponding to humid and arid conditions, i.e. $r_{clim} = 60$ s m^{-1} and $r_{clim} = 123$ s m^{-1}, respectively. Changes in area-average, open-water, reference crop, and pan evaporation caused by small regional changes in these weather variables, though broadly of the same order of magnitude, all differ to some extent. As expected, the rate of change in area-average evaporation caused by changes in weather variables falls as area-average surface resistance increases, but changes in the other estimated evaporation rates are not affected. The relationship between changes in evaporation and changes in available energy and VPD is not affected by atmospheric aridity but those in response to changes in temperature and wind speed are affected. The change in area-average evaporation rate with wind speed (Figure 1(e,f)) is noteworthy in that can be either negative or positive depending on area-average surface resistance.

5. Changes in actual evaporation rates due to ABL coupling

Type (b) changes in evaporation include, for example, the impact of changes in the area-average surface energy balance on ABL turbulence (and hence near-surface wind speed) and on surface solar radiation via changes in boundary-layer cloud cover. Later we discuss experimental evidence that indicates feedback between surface energy balance and wind speed and radiation can contribute to observed changes (Roderick *et al.*, 2007) in pan evaporation. However, linkage via ABL processes to these two weather variables has received little attention in the past, while linkage via VPD has been extensively discussed. It is the theoretical basis for this last Type (b) feedback which is the primary focus of attention below.

5.1. Coupled surface – atmosphere interactions

Experiments with coupled models of the interaction between the land surface and overlying atmosphere (McNaughton, 1976; De Bruin, 1983, 1989; McNaughton and Spriggs, 1986, 1989; Raupach, 2000, 2001) have provided understanding of how surface controls interact with ABL processes to control area-average evaporation. These modelling studies suggest that for well-watered grassland and agricultural crops in a humid climate, area-average evaporation is within 10–15% of the estimate given by the Priestley – Taylor equation with $\alpha = 1.26$, but these studies do not support the CE relationship (Bouchet, 1963). Nonetheless, it is plausible that pan evaporation will be less if area-average actual evaporation increases either because the air in the ABL is moister or because the sensible heat flux and entrainment of warm overlying air into the ABL is less and the air cooler.

McNaughton and Spriggs (1989), hereafter referred to as M&S, modelled the diurnal behaviour of surface-energy exchanges and growth of the ABL using a model which included representation of surface-energy exchange via the P-M equation and the entrainment of drier and (in potential temperature terms) warmer air in the free atmosphere overlying the inversion that defines the ABL. ABL growth was parametrized as proportional to surface sensible heat flux and inversely proportional to the strength of the inversion. Their model was initiated and validated using nine days of data from a tower at Cabauw in the Netherlands (Driedonks, 1981, 1982), which included days both with very weak and very strong inversions. Observed profiles of potential temperature and specific humidity measured at 0545 local time were used to initiate the model profiles and the measured time series of net radiation minus soil heat flux used to force surface energy balance (growth of boundary-layer cloud was not simulated). Surface evaporation calculated by the model with different prescribed values of average surface resistance were averaged over the daytime hours when the ABL was growing, along with values calculated using the Penman equation and by Equation (4) over the same time period using the available energy used in the model. When evaluating the CE hypothesis, potential evaporation was estimated from the Penman equation with available energy set equal to that used in the P-M equation. For each value of prescribed area-average surface resistance, the effective value of the parameter α in Equation (4) was calculated from the modelled daytime evaporation and the available energy, and the validity of CE hypothesis was evaluated on each of the nine days modelled.

DOI: 10.1002/qj

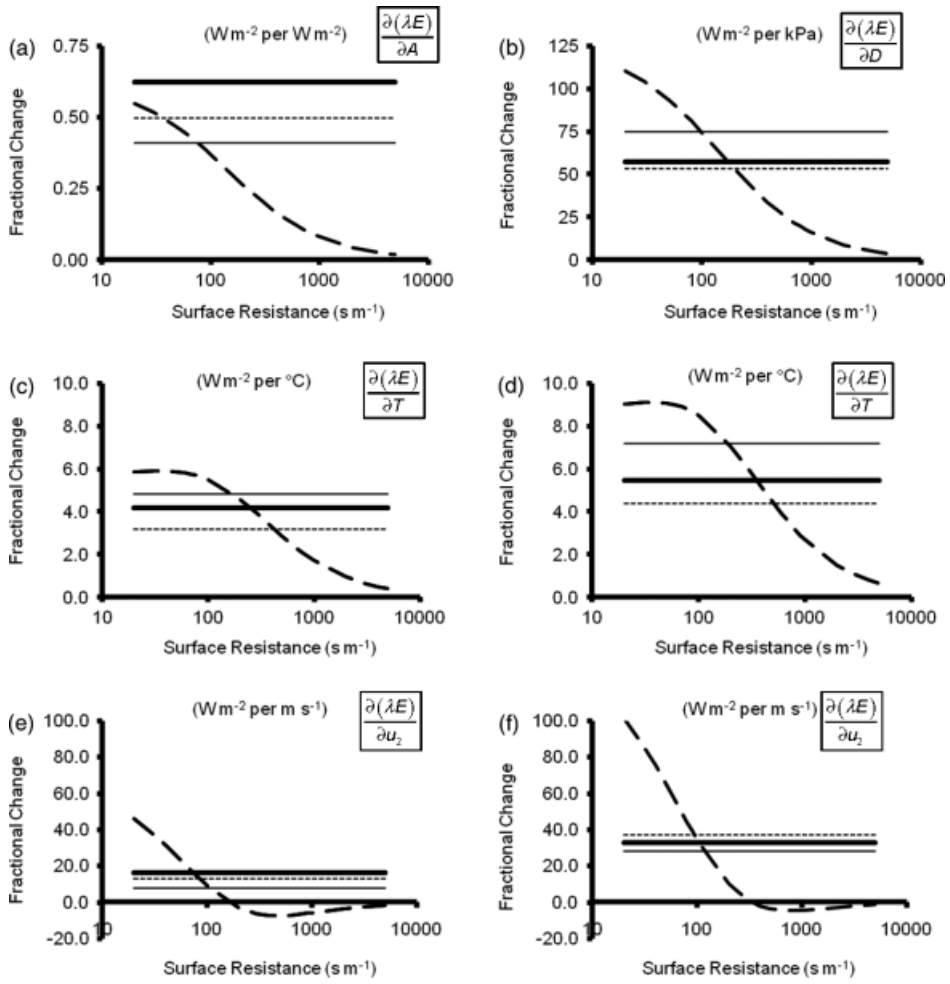

Figure 1. Fractional change in evaporation rates in response to small regional changes in (a) available energy, (b) vapour pressure deficit, (c) and (d) temperature, and (e) and (f) wind speed, all plotted as a function of the area-average surface resistance and calculated when the available energy for vegetated surfaces is 200 W m^{-2}, the 2 m temperature is 15°C, and wind speed is 2 m s^{-1}, and for vapour pressure deficit corresponding to humid ($r_{clim} = 60$ s m^{-1}) in (c) and (e), and arid conditions ($r_{clim} = 123$ s m^{-1}) in (d) and (f). The thick broken line denotes area-average evaporation, the thick full line open water evaporation, the thin broken line reference crop evaporation, and the thin full line pan evaporation.

The primary results of the M&S study can be summarized as follows.

A. The values of α calculated as a function of surface resistance on the nine days studied (reproduced in Figure 2) show substantial day-to-day variability that arguably reflects real-world variability. For surface resistance up to a few hundreds (s m^{-1}), values of α differ by approximately ±10% but above this differences are ±20–30%. Notwithstanding this variability:

   (i) For surface resistances around 70 s m^{-1}, the variation in α is moderated by a negative feedback between ABL height and evaporation. In the model (and in reality), evaporation has limited impact on absolute humidity near the surface because surface evaporation is mainly moved upwards to moisten dry air entrained into the growing ABL. However, at constant available energy, lower evaporation due to higher surface resistance results in more sensible heat and more entrainment of warm air through the inversion. As a result, VPD (and therefore evaporation) tends to increase to counteract the initial decrease in evaporation. This negative feedback moderates the extent to which α, $(\lambda E)_{aa}$ and, most important in the present analysis, D change as a function of $(r_s)_{aa}$.

   (ii) Values of α are consistent to within about ±15% of surface resistances up to about 120 s m^{-1} but the daytime average value of α when surface resistance is 70 s m^{-1} is about 8% less than 1.26. The significance of this is discussed below.

   (iii) Beyond a surface resistance of 120 s m^{-1}, α falls off progressively, initially fairly linearly but for values of surface resistance above 1000 s m^{-1} the rate of fall lessens as the limiting value ($\alpha = 0$) is approached.

B. The M&S study did not support the numerical accuracy of the Bouchet (1963) CE relationship

DOI: 10.1002/qj

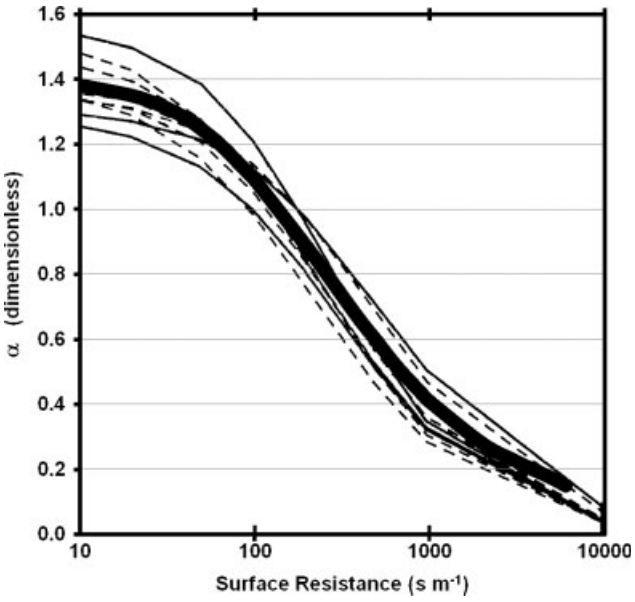

Figure 2. Day-time average values of the parameter α in the Priestley–Taylor equation as calculated as a function of surface resistance for nine days by the M&S study using a coupled model of the interaction between the land surface and the atmospheric boundary layer that was initiated and validated using field data observations made at Cabauw, Netherlands. Also shown as the thick line is the fifth-order polynomial fit to the mean value from the nine days, see Equation (10). Note that the functional form given in the text and used in calculations in this study was renormalized to give $\alpha = 1.26$ when the surface resistance is 70 s m^{-1}. (Redrawn from McNaughton and Spriggs (1989) by permission of IAHS Press).

as a general description of the strength of the feedback between modelled surface energy balance and potential evaporation. The extent of inaccuracy strongly depended on ambient meteorological conditions and, most importantly, on the strength of the inversion, with most error when the inversion was weak with entrainment and ABL growth greatest.

Although the range of environmental conditions sampled in the M&S study are limited and the universality of the calculated relationship between α and surface resistance (Figure 2) therefore open to question, and although there was substantial day-to-day variability in the relationship demonstrated, it is instructive to parametrize the average behaviour M&S found and to use this to explore the relationship between long-term changes in area-average and pan evaporation. However, first it is necessary to consider why the average value of α reported by M&S for a surface resistance of 70 s m^{-1} was less than 1.26, the value proposed by Priestley and Taylor (1972) for all-day average values of evaporation and available energy.

The M&S study calculated the average value of α during daylight hours when surface exchanges and ABL growth was active. The value α_{day} that M&S report is therefore normalized to the average net radiation during the n_{day} daylight hours modelled rather than all-day average net radiation. Since most evaporation happens during the day, $\alpha_{\mathrm{M\&S}}$, the true all-day average value, can be estimated by multiplying α_{day} by the ratio of the (higher) daytime average net radiation to the (lower) all-day average net radiation. Assuming the net long-wave radiation flux, L_{n}, is negative and constant through both day and night, then:

$$\alpha_{\mathrm{M\&S}} = \frac{[S(1-0.23) + (n_{\mathrm{day}} L_{\mathrm{n}})/24]}{[S(1-0.23) + L_{\mathrm{n}}]} \alpha_{\mathrm{day}}. \qquad (9)$$

Substituting $A_{\mathrm{veg}} = (1-0.23)S + L_{\mathrm{n}}$ into Equation (9) and assuming $A_{\mathrm{veg}} = 200$ W m^{-2}, $L_{\mathrm{n}} = -50$ W m^{-2} and $n_{\mathrm{day}} = 16$ hours, implies that an upward correction of $\sim$8% is required to renormalize the daytime relationship between modelled evaporation and net radiation calculated by M&S to the equivalent all-day relationship. For this reason, but primarily for consistency with the often-used value of α in the P-T equation, in this analysis the values of α given by M&S were normalized upwards for all values of surface resistance such that the 9-day average value of $\alpha_{\mathrm{M\&S}}$ when surface resistance is 70 s m^{-1} was increased from 1.18 to 1.26. A fifth-order polynomial fit was then made to the resulting normalized relationship between the 9-day mean values of $\alpha_{\mathrm{M\&S}}$ and area-average surface resistance which has the form:

$$\begin{aligned}\alpha_{\mathrm{M\&S}} = {} & 1.26 - 0.24141 \left[\ln\left(\frac{(r_{\mathrm{s}})_{\mathrm{aa}}}{70}\right)\right] \\ & -0.07199 \left[\ln\left(\frac{(r_{\mathrm{s}})_{\mathrm{aa}}}{70}\right)\right]^2 + 0.0099 \left[\ln\left(\frac{(r_{\mathrm{s}})_{\mathrm{aa}}}{70}\right)\right]^3 \\ & +0.00504 \left[\ln\left(\frac{(r_{\mathrm{s}})_{\mathrm{aa}}}{70}\right)\right]^4 - 0.00083 \left[\ln\left(\frac{(r_{\mathrm{s}})_{\mathrm{aa}}}{70}\right)\right]^5. \end{aligned} \qquad (10)$$

The thick line shown in Figure 2 illustrates the form of this fitted relationship but with the upward renormalization (just described) removed, so that it can be directly compared with the original results given by M&S. Confidence in this fitted relationship is particularly low at low and high values of area-average surface resistance, therefore results based on it are later shown only for $(r_{\mathrm{s}})_{\mathrm{aa}}$ in the range 20–3000 s m^{-1}.

It is important that the function $\alpha_{\mathrm{M\&S}}$ can be used to calculate the average behaviour of the VPD in the ABL in response to imposed changes in area-average surface resistance, because it is the impact of such changes in D on pan and open-water evaporation that are the basis of the interrelationship between area-average, pan and open-water evaporation sought here. Starting from the general form of the P-M equation, the behaviour of D can be derived from

$$\frac{\Delta A_{\mathrm{veg}} + (\rho c_p D)/(r_{\mathrm{a}})_{\mathrm{aa}}}{\Delta + \gamma[1 + (r_{\mathrm{s}})_{\mathrm{aa}}/(r_{\mathrm{a}})_{\mathrm{aa}}]} = \alpha_{\mathrm{M\&S}} \frac{\Delta}{\Delta + \gamma} A_{\mathrm{veg}} \qquad (11)$$

rearranged into the form:

$$D = \frac{\Delta A_{\mathrm{veg}}}{\rho c_p} \left[\frac{\alpha_{\mathrm{M\&S}} \gamma (r_{\mathrm{s}})_{\mathrm{aa}}}{\Delta + \gamma} + (\alpha_{\mathrm{M\&S}} - 1)(r_{\mathrm{a}})_{\mathrm{aa}}\right]. \qquad (12)$$

DOI: 10.1002/qj

5.2. Relating changes in area-average, pan, and open-water evaporation

For a given value of $(r_s)_{aa}$ and equivalent value of $\alpha_{M\&S}$ from Equation (10), the value of D can be calculated from Equation (12) and λE_{pan} and λE_{ow} then calculated using appropriate values of r_a, r_s, and a from Table I. Figures 3(a) and (b) show example comparisons between the variation with $(r_s)_{aa}$ of λE_{aa} and λE_{pan} while Figures 3(c) and (d) show similar comparisons between λE_{aa} and λE_{ow}. In each figure the value of λE_{comp} is also shown, with λE_{comp} defined by the equation:

$$\lambda E_{comp} = 2(\lambda E_{aa})_{70} - \lambda E_{aa}, \tag{13}$$

where $(\lambda E_{aa})_{70}$ is the value of λE_{aa} when area-average surface resistance is 70 s m^{-1}. All of the example calculations shown in Figure 3 are for wind speed 2 m s^{-1}, air temperature 15°C, and A_{veg} 200 W m^{-2}, with A_{pan} and A_{ow} calculated to allow for differences in albedo (Table I) assuming $L_n = -50$ W m^{-2} for each evaporating surface. To illustrate the sensitivity to the assumed value of area-average crop height, in Figures 3(a) and (b) three estimates of D are made from Equation (12) and used to calculate λE_{pan} and λE_{ow} with aerodynamic surface resistances corresponding to area-average vegetation heights of 0.25, 0.5 and 1.0 m. Decreasing or increasing area-average crop height does not change the main conclusions of this analysis substantially. Similarly, in Figures 3(c) and (d), three estimates of D are made and used to calculate λE_{pan} and λE_{ow} with $\alpha_{M\&S}$ given by Equation (10) and by values of $\alpha_{M\&S}$ which are 10% above and below this value. Assuming values of α which are 10% higher or lower than $\alpha_{M\&S}$ mainly alters the offset of λE_{pan} and λE_{ow} with respect to λE_{aa} but also does not change the main conclusions of this analysis. Consequently, hereafter calculations are made with $h_{aa} = 0.5$ m and $\alpha_{M\&S}$ calculated by Equation (10).

It is relevant later that, if pan evaporation is adequately estimated by the PenPan equation and area-average evaporation calculated by the P-M equation, the pan constant, $K_p(= \lambda E_{rc}/\lambda E_{pan})$, is calculable from:

$$K_p = \frac{(r_a)_{aa} + r_{clim}}{(A_{pan}/A_{aa})(r_a)_{pan} + r_{clim}} \times \frac{(\Delta + 2.4\gamma)(r_a)_{pan}}{\Delta(r_a)_{aa} + \gamma[(r_a)_{aa} + (r_s)_{aa}]}. \tag{14}$$

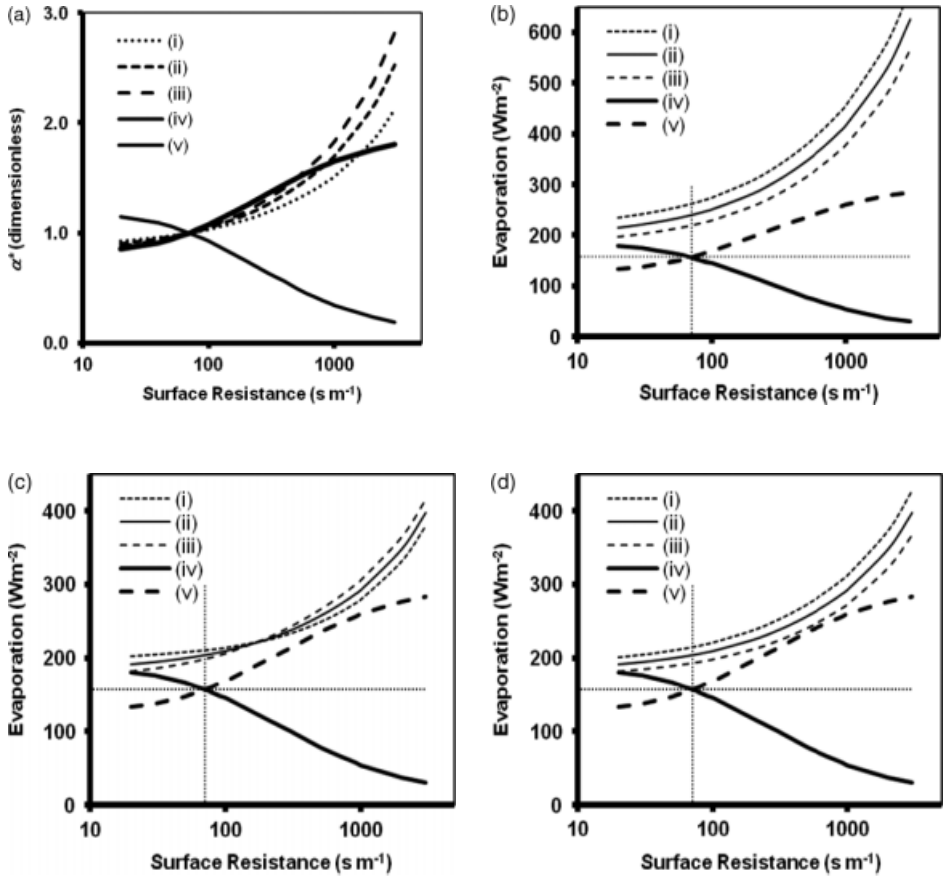

Figure 3. Variation as a function of area-average surface resistance of λE_{pan} and λE_{ow} calculated using the Penman Equation when $A_{veg} = 200$ W m^{-2}, wind speed 2 m s^{-1}, temperature 15°C, with vapour pressure deficit calculated using Equation (12). (a) shows evaporation rates calculated with different aerodynamic resistances corresponding to effective area-average vegetation heights of (i) 0.12 m, (ii) 0.5 m (the preferred value assumed in this analysis), and (iii) 1 m, respectively; and (b) shows evaporation rates calculated with an area-average vegetation height of 0.5 m but with α set to be (i) 10% less than $\alpha_{M\&S}$, (ii) equal to $\alpha_{M\&S}$, and (ii) 10% more than $\alpha_{M\&S}$, respectively. In both (a) and (b), λE_{pan} is compared with (iv) λE_{aa} and (v) λE_{comp}. Figures (c) and (d) are equivalent to (a) and (b) but for λE_{ow} (instead of λE_{pan}) calculated in the same conditions.

DOI: 10.1002/qj

Consequently, if measured pan evaporation, wind speed, and temperature are available and (A_{pan}/A_{aa}) can be estimated, changes in pan evaporation can be related to changes in area-average evaporation for specified values of climatological and area-average surface resistance. With the form assumed for the several resistances in this analysis, $K_p \sim 0.8 \pm 0.15$ for moderate wind speeds (1 to 3 m s^{-1}) and moderate temperatures (10 to 30°C) depending on atmospheric aridity, this value being typical of that determined empirically in moderate conditions (Stanhill, 1976).

If λE_{aa} and λE_{comp} are normalized to the value of λE_{aa} when the area-average surface resistance is 70 s m^{-1}, and λE_{pan} and λE_{ow} are also normalized to their respective values when D is calculated from Equation (12) using this same value of λE_{aa}, the evaporation rates λE_{aa}, λE_{comp}, λE_{pan} and λE_{ow} can be expressed in dimensionless form as $\alpha_{aa}{}^*$, $\alpha_{comp}{}^*$, $\alpha_{pan}{}^*$, and $\alpha_{ow}{}^*$. (Recall that with the parametrization of $\alpha_{M\&S}$ adopted here, $\lambda E_{aa} = (\lambda E_{PT})_{1.26}$ when the area-average surface resistance is 70 s m^{-1}.) Normalizing evaporation in this way has the advantage that the interrelationship between evaporation rates becomes less sensitive to differences in available energy for the evaporating surfaces and, in the case of pan evaporation, also less sensitive to the wind speed dependency of K_p in Equation (14).

Figure 4(a) shows the variation in $\alpha_{comp}{}^*$ and $\alpha_{pan}{}^*$ as a function of $(r_s)_{aa}$ with $A_{veg} = 200$ W m^{-2} and temperature 15°C for wind speeds of 1, 2, and 3 m s^{-1}, and Figure 4(b) shows equivalent variations but for a temperature of 25°C. In Figures 4(c) and (d), $\alpha_{pan}{}^*$ is expressed as a function of $\alpha_{comp}{}^*$. The relationships shown in Figures 4(c) and (d) are important in the context of the discussion of the CE hypothesis (see next section). Figure 4(a) shows that, when CE and pan evaporation rates are expressed in dimensionless form, they are reasonably similar for values of area-average surface resistance less than 1000 s m^{-1} at moderate temperatures ~15°C and wind speeds ~2 m s^{-1}. However, at 25°C the rate of change of pan evaporation with area-average surface resistance is much less than CE when area-average surface resistance is less than (say) 1000 s m^{-1}. Presumably this is due to feedback processes moderating the change in VPD. Ultimately at very high values of $(r_s)_{aa}$ when area-average evaporation is suppressed, the rate of change in pan evaporation with $(r_s)_{aa}$ substantially exceeds that in CE regardless of temperature because surface energy is mainly partitioned into sensible heat and the VPD in the ABL rises.

5.3. Complementary evaporation hypothesis

The theoretical link between area-average and pan evaporation rates has hitherto been expressed using the hypothetical *complementary relationship* proposed by Bouchet (1963) which in its most recent implementation (e.g. Kahler and Brutsaert, 2006) takes the form:

$$b(\lambda E_{aa} - \lambda E_p) = (\lambda E_p - \lambda E_{pan}), \qquad (15)$$

where the factor b is an empirical 'enhancement factor'. If Equation (15) were correct, and if λE_p could be defined and calculated and b determined, small changes in λE_{aa} would be inversely related to small changes in λE_{pan} in all atmospheric conditions. In Equation (15), λE_p, the 'potential' evaporation rate, is the area-average evaporation rate when the vegetation and soil in the landscape is amply supplied with moisture. However, because the phrase 'amply supplied with water' is imprecise, definition of potential evaporation rate is largely a matter of personal preference. Some authors (e.g. Kahler and Brutsaert, 2006) assume λE_p can be empirically related to a fixed multiple of the measured pan evaporation rate in conditions when the landscape is moist. Other authors (e.g. McNaughton and Spriggs, 1989) assumed λE_p is estimated by substituting A_{veg} for A_{ow} in the Penman equation, while others (e.g. Szilagyi *et al.*, 2001) assumed λE_p is estimated from a 'Penman-like' equation with A_{veg} again substituted for A_{ow} but with $(r_a)_{ow}$ replaced by Equation (2), with d and z_0 selected such that calculated evaporation in humid conditions is equal to that calculated by Equation (4) with $A = A_{veg}$ and $\alpha = 1.26$. This replacement aerodynamic resistance corresponds to a crop height of 0.007 m. The confusion regarding the definition of λE_p illustrates well what confusion can easily arise when potential evaporation rates with imprecise definition and parametrization are used as a basis of evaporation theory. The present study therefore meticulously avoids the concept of potential evaporation and is instead based only on specified actual evaporation rates.

It is instructive to contrast the theoretical description of the relationship between area-average evaporation and pan evaporation provided here with that based on the CE hypothesis. The recent paper of Kahler and Brutsaert (2006) is selected for this comparison. Here we assume that near-surface VPD (which controls pan evaporation when surface radiation and wind speed are specified) is determined by surface – ABL coupling as parameterized by the relationship between α and area-average surface resistance modelled by McNaughton and Spriggs (1989). Changes in area-average evaporation give rise to calculable changes in near-surface VPD (Equation 12) and cause calculable changes in the pan evaporation given by the PenPan equation. Kahler and Brutsaert (2006), on the other hand, assume that when area-average evaporation is less/greater than a prescribed value (given by Equation (4) with locally calibrated value of $\alpha = \alpha_e$), pan evaporation is increased/decreased by an amount that, regardless of meteorological conditions, is always equal to the reduction/increase in area-average evaporation rate multiplied by the factor b. They estimated b to be 4.33 and 6.88 using data from two sites. Kahler and Brutsaert (2006) further assume that when the landscape is plentifully supplied with moisture (broadly equivalent to assuming $(r_s)_{aa} \sim 70$ s m^{-1} in the present analysis), area-average evaporation can be estimated by multiplying measured pan evaporation by a fixed pan coefficient which they set equal to unity in all atmospheric conditions.

DOI: 10.1002/qj

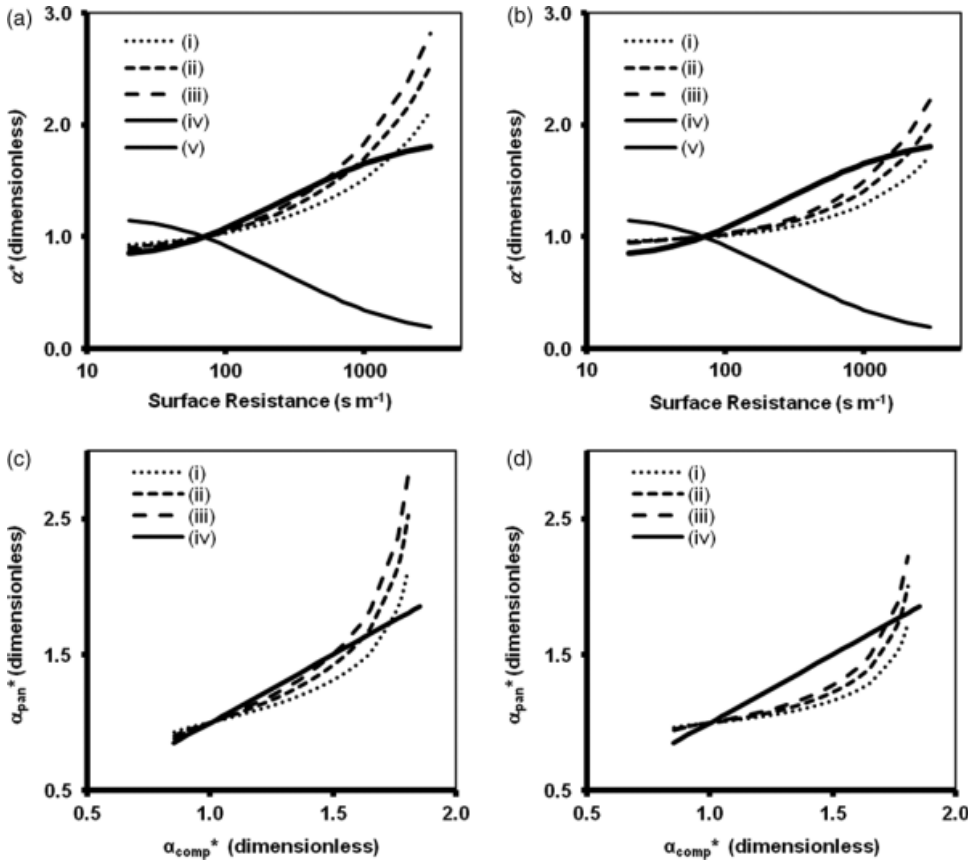

Figure 4. (a) shows the variation as a function of $(r_s)_{aa}$ of (i) $\alpha_{aa}{}^*$, (ii) $\alpha_{comp}{}^*$, and $\alpha_{pan}{}^*$ at wind speeds of (i) 1 m s^{-1}, (ii) 2 m s^{-1}, and (iii) 3 m s^{-1}, when $A_{veg} = 200$ W m^{-1} and temperature 15°C. (b) is as (a), but with calculations made at 25°C. (c) shows the variation as a function of $\alpha_{comp}{}^*$ of $\alpha_{pan}{}^*$ at wind speeds of (iii) 1 m s^{-1}, (iv) 2 m s^{-1}, and (v) 3 m s^{-1}, respectively, again calculated when $A_{veg} = 200$ W m^{-1} and temperature 15°C. (d) is as (c), but with calculations made at 25°C. In (c) and (d), (iv) illustrates the 1:1 line. (Note that changes in the value of A_{veg} do not greatly alter the general form of (a), (b), (c) and (d)).

Thus, there are marked inconsistencies between the assumptions made by Kahler and Brutsaert (2006) and the assumptions made and the results derived in the present analysis that merit highlighting. The assumption that pan evaporation is estimated by the PenPan equation, and that area-average evaporation calculated by the P-M equation gives Equation (14), indicates that the pan coefficient, rather than being a constant equal to unity, is a function of wind speed, temperature, the albedo of the pan and landscape, and area-average surface resistance. The consequent difference between pan and area-average evaporation rates when $(r_s)_{aa} = 70$ s m^{-1} is apparent in Figure 3, and allowing for this difference is required to derive the normalized evaporation rates shown in Figure 4. Further, it is apparent from Figure 4 that when the Type (b) ABL coupling processes are considered, the value of b varies with wind speed, temperature, and area-average surface resistance. It is lower at lower temperatures and higher at higher temperatures and it is typically much less than the values reported by Kahler and Brutsaert. Perhaps prescribing a fixed pan coefficient of unity was in part responsible for the high empirical values of b that Kahler and Brutseart report from their calibration.

6. Experimental evidence

6.1. Simultaneous Type (a) and Type (b) contributions to evaporative change

Recently, a new dataset has been developed that permits a first attempt at separately quantifying the relative size of Type (a) and Type (b) contributions to pan evaporation change. Specifically, several papers have now shown that near-surface wind speed has, on average, decreased across Australia (Roderick *et al.*, 2007; Rayner, 2007, McVicar *et al.*, 2008). This trend has been identified as the dominant reason for declining pan evaporation in Australia (Roderick *et al.*, 2007; Rayner, 2007) and declining wind speed has also been found important for the decline in pan evaporation in the USA, China, Canada and elsewhere (Roderick *et al.*, 2009). Such large-scale changes in wind speed (and other) weather variables imply the presence of regional-scale influences on changes in pan evaporation, here called Type (a) changes. Roderick *et al.* (2007) used the PenPan model to partition the observed changes in pan evaporation at 41 sites (1975–2004) across Australia into changes due to radiation, temperature, VPD and wind speed. The results showed that, while large-scale changes in wind speed and to a lesser extent radiation were the main influences on the observed

DOI: 10.1002/qj

changes in pan evaporation, there were also significant site-to-site differences. In some part, these site-to-site differences merely reflect experimental variability, but they also show a systematic relationship with changes in local precipitation, which is arguably a surrogate measure of changes in nearby area-average evapotranspiration (see below). Here we assume that the systematic portion of the observed site-to-site variability in pan evaporation reflects real landscape-scale Type (b) contributions to changes in pan evaporation and investigate the relative magnitude of Type (a) and (b) changes when operating via changes in radiation, wind speed, VPD and temperature.

In semi-arid and arid regions, like those covering most of Australia, evaporation is generally limited by water availability and the time-average reference crop evaporation is usually several times (perhaps 5–10 times) the time-average precipitation. When averaged over large areas, runoff is very low and although some portion (say 5–10%) of precipitation may be used for natural aquifer recharge, the vast majority of the precipitation initially entering the soil is ultimately lost as evapotranspiration (Scott *et al.*, 2000; Walvoord *et al.*, 2002, 2003; Walvoord and Phillips, 2004, Goodrich *et al.*, 2004). Because over longer periods almost all precipitation is evaporated, the long-term trend in precipitation is a reasonable surrogate measure of changes in area-average evaporation in the mainly semi-arid climates of Australia. In the following we therefore use the rate of change of measured precipitation at pan sites as a surrogate measure of the rate of change of area-average evaporation.

Thus, if the precipitation input to a semi-arid region decreases/increases, area-average evaporation will be lower/higher. If there is less/more evaporation, it might be anticipated that the VPD will rise/fall, and it is also possible there may be less/more cloud cover and an ensuing increase/decrease in surface solar radiation. Also, if precipitation (and therefore evaporation) decreases/increases in semi-arid regions, more/less surface energy will be input as sensible heat into the ABL. Wind speed is usually measured as a scalar quantity with cup anemometers, so the measured value includes a (regional-scale) vector component and a (landscape-scale) turbulent component, with the turbulent component more significant at low wind speeds. Consequently, if precipitation and evaporation decreases/increases and sensible heat increases/decreases, there will be increased/decreased buoyancy and turbulence in the ABL and the measured scalar wind speed will likely increase/decrease. It is also possible that this increased/reduced sensible heat will change the temperature of the ABL directly or indirectly by changing the input of warm air from above the inversion. All of the associated changes just described are Type (b) changes that will be superimposed on the Type (a) changes in each of the near-surface weather variables (radiation, wind speed, VPD, and temperature) that control pan evaporation.

Figures 5(a), (c), (e) and (g) respectively show the relationship between the time-average change in radiation, wind speed, VPD, and temperature relative to the time-average change in precipitation rate at the 41 sites analyzed by Roderick *et al.* (2007). Note that, while there is much scatter reflecting real-world variability, the linear regression passes close to the origin except in the case of wind speed (Figure 5(c)), where there is intercept of about -0.01 m s^{-1} yr^{-1}. The precipitation trend, averaged across all 41 sites is very close to zero ($\overline{\partial P/\partial t} = -0.03$ mm yr^{-2}), hence the intercept in Figure 5(c) is also the trend in wind speed averaged across all 41 sites. The partitioning of the trend in pan evaporation into separate components due to trends in radiation, wind speed, VPD and temperature via the PenPan model (Roderick *et al.*, 2007) relative to the precipitation trend is shown in Figures 5(b), (d), (f) and (h). In each of these figures, the intercept of the fitted relationship when the change in precipitation is zero is a measure of the net Australia-wide average Type (a) change in pan evaporation that is sampled at these 41 sites. On the other hand, the average gradient of the fitted relationship in Figures 5(b), (d), (f) and (h) is a measure of the all-site average relative strength at these 41 sites of the Type (b) feedback processes that affect pan evaporation through changes in surface radiation, wind speed, VPD, and temperature, respectively. The gradients make intuitive sense, in that they imply that more precipitation means less radiation (Figure 5(b)), and lower VPD (Figure 5(f)), for example. Interestingly, the gradients also imply that more precipitation is associated with less wind (Figure 5(d)), presumably because ABL turbulence is less. The net average observed change in pan evaporation at these 41 sites is the sum of the contributions to the change in annual pan evaporation shown in Figures 5(b), (d), (e) and (f) for the observed multi-site average rate of change in precipitation ($\overline{\partial P/\partial t} = -0.03$ mm yr^{-2}).

Table II gives the values of the Type (a) changes for radiation, wind speed, VPD, and temperature averaged over the 41 sites, the relative strengths of Type (b) changes for radiation, wind speed, VPD, and temperature averaged over the 41 sites in response to changes in precipitation (and, it is assumed, area-average evaporation), and their relative contributions to the total change in average pan evaporation for the observed site-average rate of change in precipitation. The net resulting change given by both Type (a) and Type (b) changes taken together are also given in Table II. It is clear that, because there is little observed change in the average precipitation for these 41 Australian sites as a whole, Type (a) effects provide most of the contribution to the net observed change. Consistent with previous results (Roderick *et al.*, 2007; Rayner, 2007; McVicar *et al.*, 2008), the largest time-average Type (a) change in pan evaporation is associated with the measured reduction in site-average wind speed, but there is a noticeable Type (a) change associated with an increase in area-average radiation. The Type (a) changes associated with changes in VPD and temperature are small. However, at the individual sites there are significant Type (b) changes superimposed on these Type (a) changes that are associated with the modifications in the surface energy budget resulting from the site-specific changes in precipitation (and hence area-average evaporation) at the sites. These Type (b) changes average out

DOI: 10.1002/qj

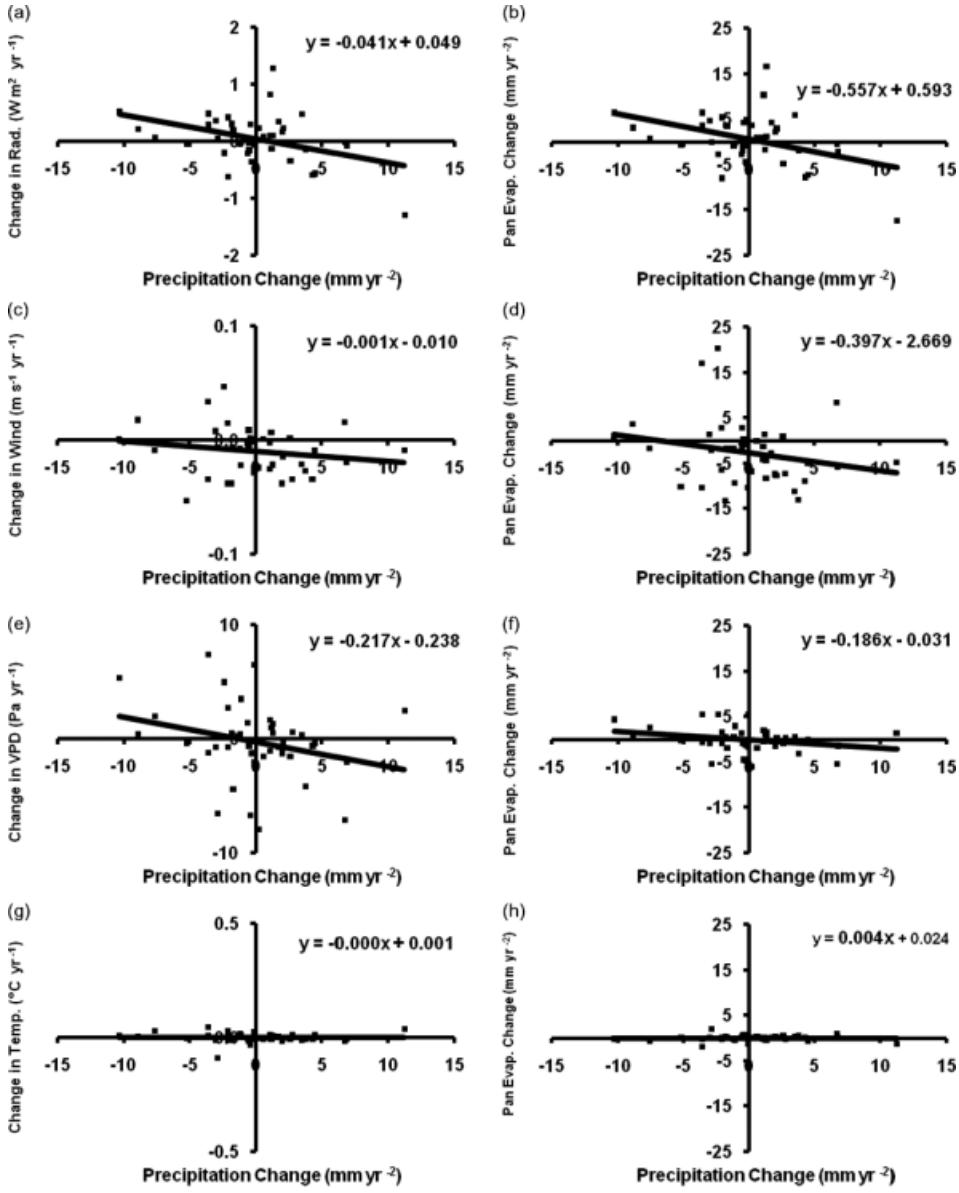

Figure 5. For the 41 Australian Class A pan sites used in the Roderick *et al.* (2007) analysis, (a), (c), (e) and (g) respectively show the relationship between the time-average change in radiation, wind speed, VPD and temperature, all relative to the change in precipitation; (b), (d), (f) and (h) respectively show the time-average change in annual pan evaporation (calculated with the Penpan equation) generated by these same changes in radiation, wind speed, VPD, and temperature relative to the change in precipitation.

over the sites because, as noted previously, the all-site average change in precipitation is very close to zero. The largest Type (b) influence is associated with changes in radiation, but there are also significant Type (b) changes associated with wind speed and VPD. It is interesting, and in the context of the CE hypothesis, significant, that the total gradient of the relationships shown in Figures 5(b), (d), (f) and (h) (column 3 in Table II) is reasonably close to unity. On the basis of Figures 4(c) and (d), this is not surprising.

6.2. Observed relationship between α and $(r_s)_{aa}$ in a semi-arid environment

Scott *et al.* (2006, 2008) gathered field measurements of surface energy, water, and carbon dioxide fluxes and associated measurements of relevant meteorological variables at three study sites representing grassland, a grassland–shrubland mosaic (hereafter referred to as a shrubland), and a mesquite woodland located on floodplain terraces along the San Pedro River in southeastern Arizona, USA. At each of these sites, data collection was maintained for several years. Herein, we use values gathered from 2003 to 2007. The measured daily total evaporation, $\lambda E_{\text{measured}}$, was expressed in terms of α_{measured} relative to the measured available energy for each crop using a Priestley – Taylor-like equation, i.e.

$$\lambda E_{\text{measured}} = \alpha_{\text{measured}} \frac{\Delta A_{\text{measured}}}{\Delta + \gamma}. \qquad (16)$$

The San Pedro River basin lies in a region that is strongly influenced by the North American monsoon system and the vegetation and surface fluxes at these

DOI: 10.1002/qj

Table II. Magnitude of Type (a) contributions to the changes in pan evaporation caused by changes in radiation, wind speed, VPD, and temperature averaged over the 41 Australian sites analyzed by Roderick *et al.* (2007), and the strength and overall magnitude of Type (b) changes in radiation, wind speed, VPD, and temperature contributions to pan evaporation averaged over these same 41 sites in response to changes in precipitation (and, it is assumed, evaporation), together with the net resulting change given by both Type (a) and Type (b) changes taken together for these 41 sites with the average observed change of −0.03 mm yr^{-2} in annual precipitation rate.

Origin of Contribution	Magnitude of Type (a) contribution (mm yr^{-2})	Strength of Type (b) contribution relative to change in precipitation (mm yr^{-2})/(mm yr^{-2})	Magnitude of Type (b) contribution (mm yr^{-2})	Net change in pan evaporation (mm yr^{-2})
Radiation	0.59	−0.56	0.02	0.61
Wind speed	−2.67	−0.40	0.01	−2.66
VPD	−0.03	−0.19	0.01	−0.03
Temperature	0.02	0.00	0.00	0.02
Total	−2.08	−1.14	0.03	−2.05

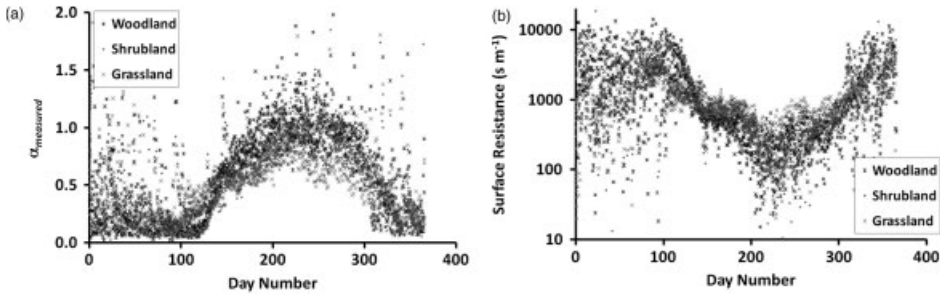

Figure 6. Daily average values of (a) $\alpha_{measured}$ and (b) surface resistance measured over several years over a woodland, shrubland, and grassland in the San Pedro River basin versus day of the year.

field sites undergo a strong seasonal variation, partly in response to the seasonal change in water availability and partly in response to the influence of weather variables, especially temperature, on the vegetation. (Frost plays a role in defining the growing season.) This pronounced seasonal variation in surface energy fluxes and associated surface resistance means these three vegetation covers provide a sample of the relationship between measured values of $\alpha_{measured}$ and surface resistance (analogous to that derived in the M&S study) for a wide range of surface resistances. The value of daily surface resistance was calculated from the measured total daily evaporation and daily average values weather variables by inverting Equation (1). Figures 6(a) and (b) respectively show all the values of $\alpha_{measured}$ and surface resistances. In Figure 6, values of $\alpha_{measured}$ that are noticeably high, and the corresponding values of surface resistance anomalously low, with respect to the general seasonal trend in these two variables correspond to days with rain. All reliable data for both dry days and days with rain or immediately after rain were included in this analysis.

Figures 7(a), (b), (c) compare the fitted curve for $\alpha_{M\&S}$ derived from the M&S modelling study (carried out in a humid environment) with the values of all-day average surface resistance and $\alpha_{measured}$ on individual days over the woodland, shrubland, and grassland vegetation cover. In all three cases, the data show substantial variability which is presumably partly due to experimental error associated mainly with shortcomings in the eddy correlation measurements of energy fluxes and estimated to be 10–15%. (Scott *et al.*, 2006, provide greater detail.). However, it is also likely that the variability in Figure 7, which is greater than this estimated experimental error, is in part a reflection of the natural variability of the atmospheric processes that couple the surface with the ABL and of the day-to-day variability in the strength of the inversion layer. Figure 7(d) shows a comparison between the fitted curve for $\alpha_{M\&S}$ and a curve obtained by fitting all the data for all of the vegetation covers, along with the standard deviation for all the individual values of $\alpha_{measured}$ that corresponded with values of surface resistance that lay in ranges 0–50, 50–100, 100–200, 200–400, 400–700, 700–1000, 1000–2000, and 2000–4000 s m^{-1}. Figure 7 shows that the relationship between α and surface resistance measured at all three field sites is consistent with $\alpha_{M\&S}$ within the (albeit large) variability present in the data.

The measured albedo and aerodynamic characteristics of the vegetation at the sites (Table III) are different to those of the area-average vegetation hitherto assumed in this analysis. Moreover, the measured weather variables available were not taken at 2 m but the equations that calculate pan and open-water evaporation rates contain empirical expressions for aerodynamic resistance that require the values of wind speed and VPD that would have been measured at 2 m by a standard weather station.

DOI: 10.1002/qj

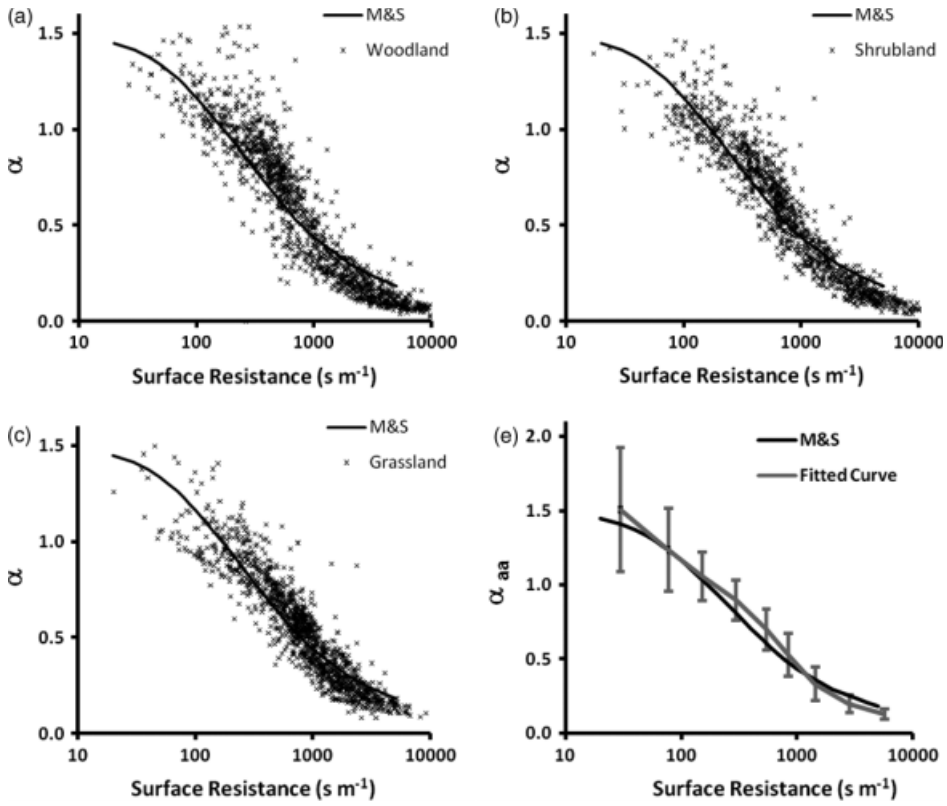

Figure 7. Comparison between the fitted curve for $\alpha_{M\&S}$ from Equation (24) and the values of all-day average surface resistance and $\alpha_{measured}$ measured on individual days for (a) woodland, (b) shrubland, and (c) grassland vegetation cover in the San Pedro River basin. (d) Comparison between the fitted curve for $\alpha_{M\&S}$ with a curve fitted to data from all of the vegetation covers in the San Pedro River basin, along with the standard deviation for all the individual values of $\alpha_{measured}$ for values of surface resistance in ranges 0–50, 50–100, 100–200, 200–400, 400–700, 700–1000, 1000–2000, and 2000–4000 s m^{-1}.

Table III. The crop height, measurement height, zero-plane displacement, aerodynamic roughness length, and albedo of the three field crops for which data were collected at San Pedro River basin field sites (from R.L. Scott, 2008, personal communication).

Variable	Units	Woodland	Shrubland	Grassland
Screen height	m	14.00	6.40	3.00
Crop height	m	7.00	3.00	1.00
Zero-plane displacement	m	4.69	2.01	0.67
Aerodynamic roughness	m	0.86	0.3769	0.123
Albedo	–	0.093	0.104	0.115

In order to make comparisons between the measured evaporation rates and calculated pan and open-water evaporation, it was therefore necessary to estimate from the available data the values of available energy, wind speed and VPD that would have been measured at 2 m above a reference crop. To do this, the approach described by Shuttleworth (2006) was modified as described in the Appendix.

Comparison between measured rates and calculated pan and open-water rates was made in terms of the normalized evaporation rates $\alpha_{aa}{}^*$, $\alpha_{comp}{}^*$, $\alpha_{pan}{}^*$, and $\alpha_{ow}{}^*$ introduced earlier. In the case of $\alpha_{aa}{}^*$ and $\alpha_{comp}{}^*$, the required value of actual crop evaporation from the natural vegetation at the field sites needed to make this normalization, denoted here as $(\lambda E_c)_{70}$, was calculated each day from the P-M equation by setting the surface resistance to 70 s m^{-1} and using the measured available energy, A_c, and the aerodynamic resistance, $(r_a)_c$, calculated from the measured wind speed and the aerodynamic characteristic of the each crop (Table III). The value of $(\lambda E_c)_{70}$ was then used to calculate the equivalent value of α_{70} from the equation:

$$(\lambda E_c)_{70} = \alpha_{70}\,\frac{\Delta A_c}{\Delta+\gamma}. \tag{17}$$

The equivalent value of VPD, D_{70}, was then calculated by setting $(r_s)_c = 70$ s m^{-1} in

$$D_{70} = \frac{\Delta A_c}{\rho c_p}\left[\frac{\alpha_{70}\gamma(r_s)_c}{\Delta+\gamma} + (\alpha_{70}-1)(r_a)_c\right]. \tag{18}$$

This value of VPD and the measured wind speed were then corrected to those required to calculate pan and open-water evaporation, see Appendix. The values of pan and

DOI: 10.1002/qj

open-water evaporation calculated using these corrected values are those required to normalize the pan and open-water evaporation.

Because the San Pedro experimental data show that specific relationships between α and surface resistance cannot be separately defined for individual vegetation covers (Figure 7), normalized values of $\alpha_{aa}{}^*$ and $\alpha_{comp}{}^*$ for all three covers and equivalent values of $\alpha_{pan}{}^*$ and $\alpha_{ow}{}^*$ were given equal status. The general relationships between $\alpha_{pan}{}^*$ and $\alpha_{ow}{}^*$ and corresponding values of $\alpha_{aa}{}^*$ and $\alpha_{comp}{}^*$ are shown without selection for ambient temperature or wind speed in Figure 8(a) and (b), respectively. This figure provides a measure of the time-average effectiveness of the CE hypothesis. In Figure 8 the rough agreement between $\alpha_{comp}{}^*$ and $\alpha_{pan}{}^*$ is arguably better than between $\alpha_{comp}{}^*$ and $\alpha_{ow}{}^*$ but recall that K_p (Equation 14) is typically less than unity and, without normalization, changes in pan evaporation in response to area-average surface resistance would be systematically higher.

Earlier it was shown that the relationship between $\alpha_{pan}{}^*$ and $\alpha_{comp}{}^*$ and $\alpha_{aa}{}^*$ changes with temperature and wind speed (Figure 4). The data shown in Figure 9 have been selected to lie around the temperatures and wind speeds used to calculate the theoretical lines shown in each case, i.e. in 10°C bands of temperature around 15°C and 25°C, and 1 m s^{-1} bands around wind speeds of 1 m s^{-1}, 2 m s^{-1} and 3 m s^{-1}. The way the theoretical relationships change with temperature and wind speed is broadly consistent with the observational data, albeit there is substantial experimental variability in the observations in part likely due to day-to-day variability in atmospheric coupling and the strength of the inversion. The consistency between theory and data is noticeably better at 25°C than at 15°C and the variability in the data much greater in the latter case. In practice, the data at 15°C correspond to periods early and late in the year, typically before day 120 and after day 300, when measured evaporation and α_{aa} are low and measured surface resistance very high, with large differences on individual days when there is rain (Figure 6). Spatial and temporal variability in surface resistance and the plot-scale advection may therefore account for much of the experimental variability shown in Figures 9(a), (c), and (d). However, it is tempting and not unrealistic to speculate that the physical processes involved in surface–ABL coupling represented in the M&S modelling study (and in reality) are relatively less influential, and the influence of day-to-day changes in the advected air mass more significant, in determining VPD when surfaces resistance is high.

7. Summary and conclusions

This paper advances the argument that there are two distinct classes of influences giving rise to changes in pan evaporation, namely Type (a) and Type (b) processes. The former are related to large-scale changes in the atmospheric circulation pattern, the latter to landscape-scale feedback between the land surface and air within the ABL. When deriving theoretical formulae describing the interrelationship between area-average and pan evaporation, actual evaporation rates defined by the Penman – Monteith equation were used in this study and hypothetical potential evaporation rates studiously avoided. The Bouchet (1963) CE hypothesis was not *a priori* assumed as the basis for describing Type (b) interaction between area-average and pan evaporation via VPD, rather the modelling results of McNaughton and Spriggs (1989) were parametrized to give an average representation of the coupling between land surfaces and the ABL. However, it is important to recognize that McNaughton and Spriggs (1989) did not include representation of all Type (b) effects. Further modelling studies that include Type (b) feedback via scalar wind speed and boundary-layer cloud cover are therefore required.

An important result of the present study is that it shows that, even when expressed in normalized form to take account of differences in the surface energy,

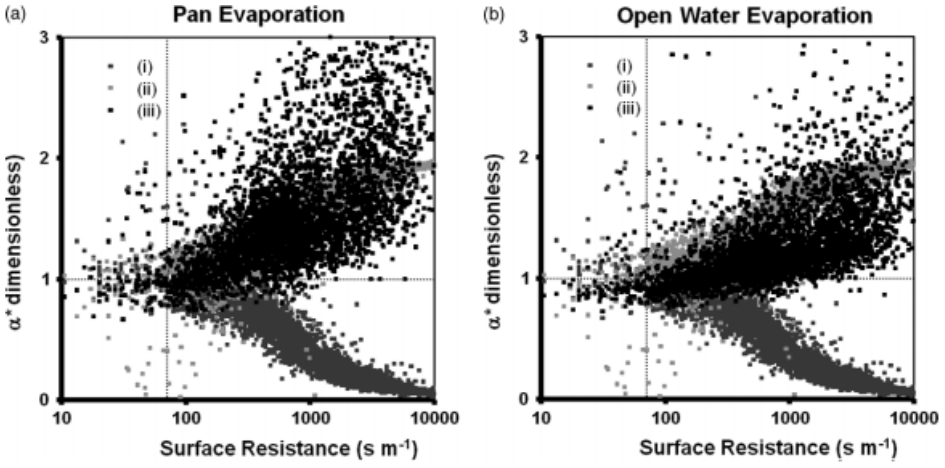

Figure 8. Comparison between (a) measured values of (i) $\alpha_{aa}{}^*$, (ii) $\alpha_{comp}{}^*$, and (iii) $\alpha_{pan}{}^*$, and (b) between measured values of (i) $\alpha_{aa}{}^*$, (ii) $\alpha_{comp}{}^*$, and (iii) $\alpha_{ow}{}^*$ calculated from the values α and surface resistance for all three vegetation covers in the San Pedro River basin measured on the individual days when field data were available without selection for ambient temperature or wind speed.

DOI: 10.1002/qj

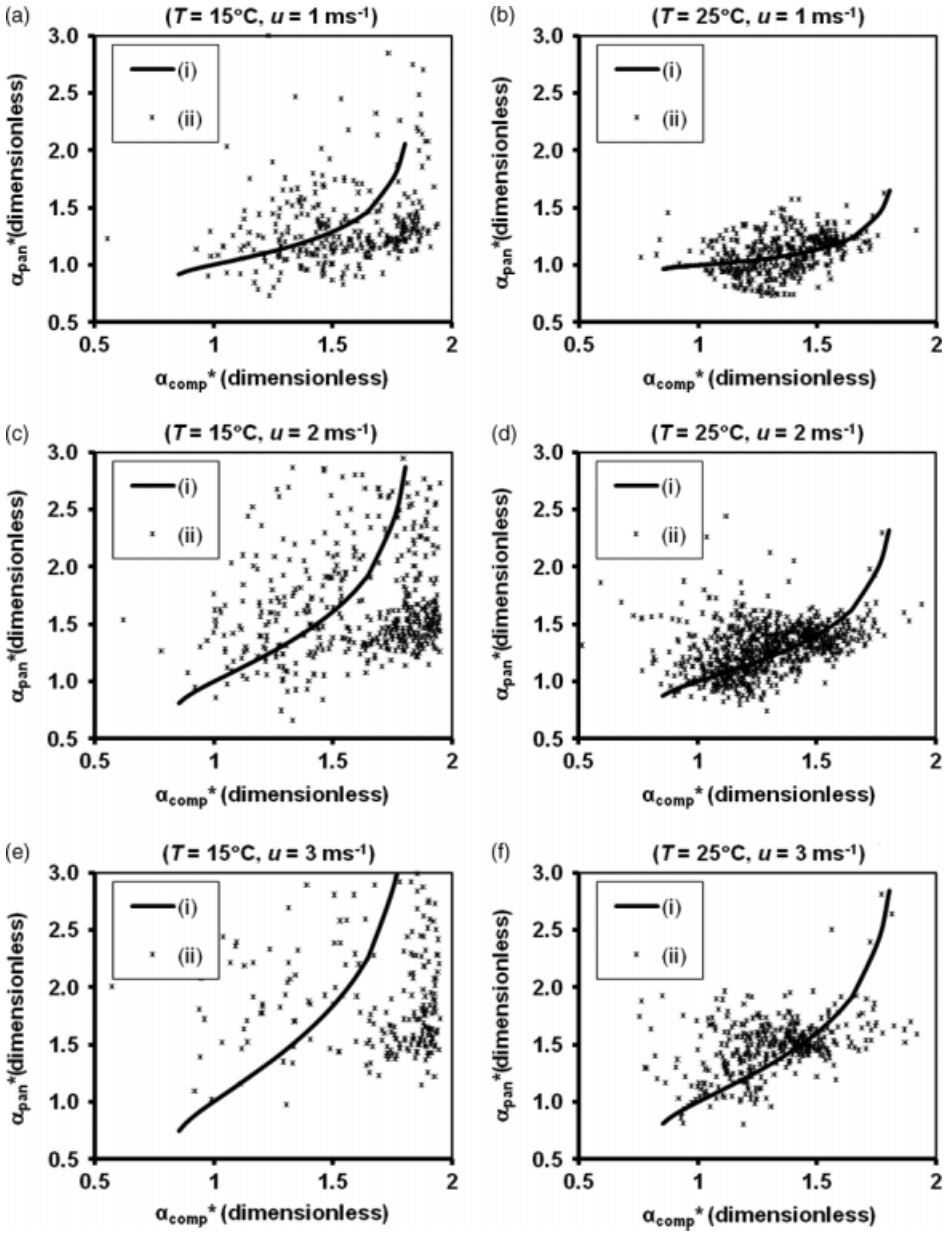

Figure 9. The theoretical relationship between $\alpha_{comp}{}^*$ and $\alpha_{pan}{}^*$ (solid line), calculated making allowance for differences in available energy with D calculated from Equation (12), and assuming the relationship between $\alpha_{M\&S}$ and surface resistance in Equation (10), for wind speed of 1 m s^{-1} at temperatures of (a) 15°C and (b) 20°C. (c, d) and (e, f) are as (a, b), but for wind speeds of 2 and 3 m s^{-1}, respectively. For comparison, the measured values of $\alpha_{comp}{}^*$ and $\alpha_{pan}{}^*$ for all three vegetation covers in the San Pedro River basin are shown as crosses, with field data selected in temperature bands 10–20°C and 20–30°C, and wind speed bands 0.5–1.5, 1.5–2.5 and 2.5–3.5 m s^{-1}.

the interrelationship between area-average and pan evaporation is not the simple linear relationship implied by the CE hypothesis. Rather the relationship varies with ambient temperature and wind speed. However, if this temperature and wind speed dependency in the relationship is ignored, the present study broadly supports an albeit very approximate inverse relationship between appropriately normalized changes in area-average and pan evaporation, though with an 'enhancement factor' which is much less than the values suggested by Kahler and Brutsaert (2006).

Already published data were reanalyzed to extract information relevant to this paper. Reanalysis of the pan evaporation dataset analyzed by Roderick *et al.* (2007) confirms the presence of Type (a) changes in pan evaporation that are associated primarily with large-scale changes in wind speed and to a lesser extent surface radiation. However, it also suggests evidence for Type (b) changes at individual sites that are associated with landscape-scale coupling between the surface and ABL via surface radiation, wind speed, and VPD. However, when averaged across all the pan data, the overall average effect of these Type (b) influences is small because, when averaged over all the pan sites in Australia, the change in precipitation and therefore in area-average evaporation is small.

Data previously reported by Scott *et al.* (2008) are reanalyzed with emphasis on investigating the validity

DOI: 10.1002/qj

or otherwise of the theory derived to describe Type (b) changes associated with surface–ABL coupling via VPD. The semi-arid setting for these observations is very different to the sub-humid conditions used to initiate the M&S modelling studies, but the average parametrization of the relationship between α and surface resistance given by M&S is consistent within the variability in the observations. Figure 8 shows that observations confirm there is some approximate similarity between ${\alpha_{\rm pan}}^*$ and ${\alpha_{\rm comp}}^*$. However, the present analysis demonstrates that this relationship changes with ambient conditions, and Figure 9 shows that there is at least reasonable agreement with theoretically predicted differences in the relationship at different temperatures and wind speeds.

On the basis of the present analysis, it is clear that the hitherto often attempted simplistic interpretation of the implications of observed changes in pan evaporation in terms of associated changes in area-average evaporation is inherently flawed. This is because (i) there are two types of influences, Type (a) and Type (b), operating at different spatial scales and usually in opposite directions, and (ii) both of these types of influence can operate through more than one of the several near-surface weather variables that control area-average and pan evaporation. As previously stated, adequate description of the relationship between changes in actual and pan evaporation rates will therefore require using models that simultaneously represent Type (a) and (b) influences in the atmosphere to realistically calculate the near-surface weather variables that control atmospheric demand. But not only this; throughout this study it is explicitly recognized that changes in area-average evaporation are controlled not only by changes in atmospheric demand, but also by changes in area-average surface resistance that reflect, among other things, changes in the moisture available at the surface. As the example of Australia well illustrates, the relationship between changes in pan and area-average evaporation depends not only on changes in radiation, wind speed, VPD and temperature, but also on changes in precipitation.

Acknowledgements

This work was supported by SAHRA (Sustainability of semi-Arid Hydrology and Riparian Areas) under the STC Program of the National Science Foundation, Agreement No. EAR-9876800 and NSF award DEB–0415977, and by JCHMR (Joint Centre for Hydro-Meteorological Research) at the Centre for Ecology and Hydrology, Wallingford, UK. MLR acknowledges the support of the Australian Research Council (DP0879763).

Appendix

Deriving 2 m variables from above-canopy measurements

The weather data available from the three field sites in the San Pedro river basin were collected at different heights above the canopy of different vegetation covers with canopy characteristics which differ significantly from those assumed elsewhere in this analysis (Table III). The equations used to estimate open-water and pan evaporation rates contain empirical expressions for aerodynamic resistance that require the value of windspeed and VPD at a height of 2 m, equivalent to the values that would have been provided by a standard weather station located above short grass nearby the field sites. To estimate these evaporation rates, it is necessary to estimate these weather variables from the data measured above the vegetation. Following Shuttleworth (2006), to do this it is assumed that there is a 'blending height' 50 m above the ground at which any differences in values of weather variables above different vegetation can be considered negligible and that there is no divergence of the net radiation, momentum, sensible heat, and latent heat fluxes between this level and the vegetation.

A.1 Available Energy

If the albedo of the the crop over which measurements are available is $a_{\rm c}$ and the available energy for this crop $A_{\rm c}$, then neglecting differences in the net long-wave radiation flux for different vegetation and selecting a typical value of $L_n = -50$ W m^{-2}, the available energy A' ($= A_{\rm veg}$; $A_{\rm pan}$; $A_{\rm ow}$) are given by substituting the corresponding values of a' ($= a_{\rm veg}$; $a_{\rm pan}$; $a_{\rm ow}$) in the equation:

$$A' = (A_{\rm c} + L_n)\frac{(1-a')}{(1-a_{\rm c})} - L_n. \qquad \text{(A.1)}$$

A.2 Wind speed

If z_0 and d are the aerodynamic roughness and zero-plane displacement of the vegetation cover above which wind speed, $u_{\rm m}$, and VPD, $D_{\rm m}$, are measured, and these measurements are made at a height $h_{\rm m}$ above the ground, then assuming no divergence of momentum flux between $h_{\rm m}$ and 50 m, the wind speed at 50m, u_{50}, is estimated by:

$$u_{50} = (u_{\rm m}).\frac{\ln[(50-d)/(z_0)]}{\ln[(h_{\rm m}-d)/(z_0)]}. \qquad \text{(A.2)}$$

Assuming the wind speed at 50 m is the same above the crop and a hypothetical area reference crop somewhere in the landscape, and using standard values of aerodynamic roughness and zero-plane displacement for a reference crop, the required wind speed 2 m above the reference crop, u_2, is:

$$u_2 = u_{50}.\frac{\ln[(2-0.08)/(0.0148)]}{\ln[(50-0.08)/(0.0148)]}. \qquad \text{(A.3)}$$

A.3 Vapour pressure deficit

For the crop above which measurements are made, the aerodynamic resistances to $h_{\rm m}$ and 50 m, ${(r_{\rm a})_{\rm c}}^{\rm m}$ and

DOI: 10.1002/qj

$(r_a)_c{}^{50}$, respectively, are estimated from Equation (2) as:

$$(r_a)_c{}^{m} = \frac{\ln\left\{\frac{(h_m-d)}{z_0}\right\}.\ln\left\{\frac{(h_m-d)}{(z_0/10)}\right\}}{k^2\ u_m}, \tag{A.4}$$

$$(r_a)_c{}^{50} = \frac{\ln\left\{\frac{(50-d)}{z_0}\right\}.\ln\left\{\frac{(50-d)}{(z_0/10)}\right\}}{k^2\ u_{50}}, \tag{A.5}$$

and the measured surface resistance of the crop is $(r_s)_c$. If there is no divergence of latent and sensible heat flux between h_m and 50 m, the evaporation calculated by the P-M equation using values appropriate to h_m and 50 m must be the same, i.e.

$$\frac{\Delta A_c + (\rho c_p D_m)/(r_a)_c{}^{m}}{\Delta + \gamma[1 + (r_s)_c/(r_a)_c{}^{m}]} = \frac{\Delta A_c + (\rho c_p D_{50})/(r_a)_c{}^{50}}{\Delta + \gamma[1 + (r_s)_c/(r_a)_c{}^{50}]}, \tag{A.6}$$

where D_{50} is the VPD at 50 m.

Rearranging Equation (A.6) gives:

$$D_{50} = \frac{\Delta A_c}{\rho c_p}\left[\left\{\frac{(\Delta+\gamma)(r_a)_c{}^{50} + \gamma(r_s)_c}{(\Delta+\gamma)(r_a)_c{}^{m} + \gamma(r_s)_c}\right\} \times \left\{(r_a)_c{}^{m} + \frac{\rho c_p D_m}{\Delta A_c}\right\} - (r_a)_c{}^{50}\right]. \tag{A.7}$$

Similarly, in the case of the reference crop the aerodynamic resistances to 2 m and 50 m, $(r_a)_{rc}{}^{2}$ and $(r_a)_{rc}{}^{50}$, respectively, are estimated by:

$$(r_a)_{rc}{}^{2} = \frac{\ln\left[\frac{2-0.08}{0.0148}\right].\ln\left[\frac{2-0.08}{0.0148}\right]}{k^2\ u_2}, \tag{A.8}$$

$$(r_a)_{rc}{}^{50} = \frac{\ln\left[\frac{50-0.08}{0.0148}\right].\ln\left[\frac{50-0.08}{0.0148}\right]}{k^2\ u_{50}}, \tag{A.9}$$

and the surface resistance of a reference crop is 70 s m^{-1}. If there is again no divergence of latent and sensible heat flux between h_m and 50 m, the reference crop evaporation calculated by the P-M equation using values appropriate to 2 m and 50 m must be the same and, D_2 the required VPD at 2 m above a reference crop is given by:

$$D_2 = \frac{\Delta A_{rc}}{\rho c_p}\left[\left\{\frac{(\Delta+\gamma)(r_a)_c{}^{2} + 70\gamma}{(\Delta+\gamma)(r_a)_c{}^{50} + 70\gamma}\right\} \times \left\{(r_a)_c{}^{2} + \frac{\rho c_p D_{50}}{\Delta A_{rc}}\right\} - (r_a)_{rc}{}^{2}\right]. \tag{A.10}$$

References

Allen RG, Pereira LS, Raes D, Smith M. 1998. 'Crop evapotranspiration'. Irrigation and Drainage Paper 56, UN Food and Agriculture Organization: Rome.

Askoy B. 1997. Variations and trends in global solar radiation for Turkey. *Theor. Appl. Climatol.* **58**: 71–77.

Bouchet RJ. 1963. Evapotranspiration réelle, evapotranspiration potentielle, et production agricole. *Ann. Agron.* **14**: 543–824.

Brutsaert W, Parlange MP. 1998. Hydrological cycle explains the evaporation paradox. *Nature* **396**(5): 284–285.

Brutsaert W. 2006. Indications of increasing land surface evaporation during the second half of the 20th century. *Geophys. Res. Lett.* **33**: L20403, DOI: 10.1029/2006GL027532.

Chattopadhyay N, Hume M. 1997. Evaporation and potential evaporation in India under conditions of recent and future climate change. *Agric. Forest Meteorol.* **87**: 55–73.

Chen D, Gao G, Xu C-Y, Guo J, Ren G. 2005. Comparison of the Thornthwaite method and pan data with the standard Penman-Monteith estimates of reference evapotranspiration in China. *Clim. Res.* **28**: 123–132.

Cohen S, Ianetz A, Stanhill G. 2002. Evaporative climate changes at Bet Dagan, Israel, 1964–1998. *Agric. Forest Meteorol.* **111**: 83–91.

De Bruin HAR. 1983. A model of the Priestley-Taylor parameter, α. *J. Appl. Meteorol.* **22**: 572–578.

De Bruin HAR. 1989. Physical aspects of the planetary boundary layer. In *Estimation of Areal Evaporation* (Black TA, Spittlehouse DL, Novak MD, Price DT. (eds.) IAHS Publication No.177, IAHS Press: Wallingford, UK.

Doorenbos J, Pruitt WO. 1977. Crop water requirements. Irrigation and Drainage Paper 24. United Nations Food and Agriculture Organization: Rome.

Driedonks AGM. 1981. Dynamics of the well-mixed atmospheric boundary layer. Scientific Report W.R. 81–82 KNMI: De Bilt, The Netherlands.

Driedonks AGM. 1982. Models and observations of the growth of the atmospheric boundary layer. *Boundary-layer Meteorol.* **23**: 283–306.

Farahani HJ, Howell TA, Shuttleworth WJ, Bausch WC. 2007. Evapotranspiration: Progress in measurement and modelling in agriculture. *Trans. Amer. Soc. Agric. Biol. Engineers* **50**(5): 1627–1638.

Gash JHC, Shuttleworth WJ. 2007. *Evaporation*. Benchmark Papers in Hydrology Series, No. 2. IAHS Press: Wallingford, UK.

Gedney N, Cox PM, Betts RA, Boucher O, Huntingford C, Stott PA. 2006. Detection of a direct carbon dioxide effect in continental river runoff records. *Nature* **439**(16): 835–837, DOI: 10.1038/nature04504.

Goodrich DC, Williams DG, Unkrich CL, Hogan JF, Scott RL, Hultine KR, Pool D, Coes AL, Miller S. 2004. Comparison of methods to estimate ephemeral channel recharge, Walnut Gulch, San Pedro River Basin, Arizona. In *Groundwater Recharge in a Desert Environment: The Southwestern United States.* Hogan JF, Phillips FM, Scanlon BR. (eds.) AGU Water Science and Applications Series, 9: 77–99.

Hobbins MT, Ramirez JA, Brown TC. 2004. Trends in pan evaporation and actual evapotranspiration across the conterminous US: Paradoxical or complementary? *Geophys. Res. Lett.* **31**: L3503. DOI: 10.1029/2004GL019846.

IPCC. 2007. *Working Group I Report: The Physical Science Basis.* Intergovernmental Panel on Climate Change. Available at http://ipcc-wg1.ucar.edu/wg1/wg1-report.html.

Jensen ME, Burman RD, Allen RG. 1990. Evapotranspiration and irrigation water requirements. *ASCE Manual* **70**: p 332.

Kahler DM, Brutsaert W. 2006. Complementary relationship between daily evaporation in the environment and pan evaporation. *Water Resour. Res.* **42**: W05413. DOI: 10, 1029/2005WR004541.

Linacre ET. 1994. Estimating US Class A pan evaporation data from few climate data. *Water Int.* **19**: 5–14.

McVicar TR, Van Niel TG, Li LT, Roderick ML, Rayner DP, Ricciardulli L, Donohue RJ. 2008. Wind speed climatology and trends for Australia, 1975–2006: Capturing the stilling phenomenon and comparison with near-surface reanalysis output. *Geophys. Res. Lett.* **35**: L20403, DOI: 10.1029/2008GL035627.

MacNaughton KG. 1976. Evaporation and advection, I: Evaporation from extensive homogeneous surfaces. *Q. J. R. Meteorol. Soc.* **102**: 181–191.

McNaughton KG, Spriggs TW. 1986. A mixed-layer model of regional evaporation. *Boundary-layer Meteorol.* **34**: 243–262.

McNaughton KG, Spriggs TW. 1989. An evaluation of the Priestley–Taylor equation. In *Estimation of Areal Evaporation.* Black TA, Spittlehouse DL, Novak MD, Price DT. (eds.) IAHS Publication No.177, IAHS Press: Wallingford, UK.

Monteith JL. 1965. Evaporation and environment. *Sympos. Soc. Exper. Biol.* **19**: 205–234.
Ohmura A, Wild M. 2002. Is the hydrological Cycle accelerating? *Science* **298**: 1345–1346.
Omran MA. 1998. Analysis of solar radiation over Egypt. *Theor. Appl. Climatol.*, **67**: 225–240.
Penman HL. 1948. Natural evaporation from open water, bare soil, and grass. *Proc. R. Soc. London* **A193**: 120–145.
Penman HL. 1963. Vegetation and hydrology. Technical Communication 53, Commonwealth Bureau of Soils: Harpenden, England.
Pereira LS, Perrier A, Allen RG, Alves I. 1999. Evapotranspiration: Concepts and future trends. *J. Irrig. Drain. Eng.* **125**(2): 45–51.
Peterson TC, Golubev VS, Groisman PY. 1995. Evaporation losing its strength. *Nature* **377**(26): 687–688.
Priestley CHB, Taylor RJ. 1972. On the assessment of surface heat flux and evaporation using large-scale parameters. *Mon. Weather Rev.* **100**: 81–92.
Ramanathan V, Crutzen PJ, Keihl JT, Rosenfeld D. 2001. Aerosols, climate and the hydrological cycle. *Science* **294**: 2119–2124. DOI: 10.1126/science.1064034.
Raupach MR. 2000. Equilibrium evaporation and the convective boundary layer. *Boundary-Layer Meteorol.* **96**: 107–141.
Raupach MR. 2001. Combination theory and equilibrium evaporation. *Q. J. R. Meteorol. Soc.* **127**: 1149–1181.
Rayner DP. 2007. Wind run changes are the dominant factor affecting pan evaporation trends in Australia. *J. Climate* **20**: 3379–3394.
Roderick ML, Farquhar GD. 2002. The cause of decreased pan evaporation over the past 50 years. *Science* **298**: 1410–1411.
Roderick ML, Farquhar GD. 2004. Changes in Australian pan evaporation from 1970 to 2002. *Int. J. Climatol.* **24**: 1077–1090.
Roderick ML, Farquhar GD. 2005. Changes in New Zealand pan evaporation from the 1970s. *Int. J. Climatol.* **25**: 2013–2039.
Roderick ML, Rotstayn LD, Farquhar GD, Hobbins MT. 2007. On the attribution of changing pan evaporation. *Geophys. Res. Lett.* **34**: L17403, DOI: 10.1029/2007GL031166.
Roderick ML, Hobbins MT, Farquhar GD. 2009. Pan evaporation trends and the terrestrial water balance II. Energy balance and interpretation. *Geography Compass* **3**(2): 761–780.
Rotstayn LD, Roderick ML, Farquhar GD. 2006. A simple pan-evaporation model for analysis of climate simulations: Evaluation over Australia. *Geophys. Res. Lett.* **33**: L17715. DOI: 17710.11029/12006GL027114.
Scott RL, Shuttleworth WJ, Keefer TO, Warrick AW. 2000. Modelling multiyear observations of soil moisture recharge in the semiarid American Southwest. *Water Resour. Res.* **36**(8): 2233–2247.
Scott RL, Huxman TE, Williams DG, Goodrich DG. 2006. Ecohydrological impacts of woody-plant encroachment: seasonal patterns of water and carbon dioxide exchange within a semiarid riparian environment. *Global Change Biology* **12**: 311–324. DOI: 10.1111/j.1365–2486.2005.01093.x.
Scott RL, Cable WL, Huxman TE, Nagler PL, Hernandez M, Goodrich DC. 2008. Multiyear riparian evapotranspiration and groundwater use for a semiarid watershed. *J. Arid Environ.* **72**: 1232–1246.
Shenbin C, Yunfeng L, Thomas A. 2006. Climatic change on the Siberian plateau: Potential evapotranspiration trends from 1961 to 2000. *Climate Change* **76**: 291–319.
Shuttleworth WJ. 1993. Evaporation. In *Handbook of Hydrology*. Maidment DR. (ed.) McGraw-Hill: New York, USA.
Shuttleworth WJ. 2006. Towards one-step estimation of crop water requirement. *Trans. Amer. Soc. Agric. Biol. Eng.* **49**(4): 925–935.
Shuttleworth WJ. 2008. Evapotranspiration measurement methods. *Southwest Hydrol.* **7**(1): 22–23. At http://www.swhydro.arizona.edu/archive/V7_N1/.
Stanhill G. 1976. *The CIMO International Evaporimeter Comparisons*. World Meteorological Organization: Geneva, Switzerland.
Stanhill G, Cohen S. 2001. Global dimming: A review of the evidence for a widespread and significant reduction in global radiation with discussion of its probable causes and possible agricultural consequences. *Agric. Forest Meteorol.* **107**: 255–278.
Szilagyi J, Katul GG, Parlange MB. 2001. Evaporation intensifies over the conterminous United States. *J. Water Resour. Plan. Manag.* **127**(6): 354–362.
Thom AS, Oliver HR. 1977. On Penman's equation for estimating evaporation. *Q. J. R. Meteorol. Soc.* **103**: 345–357.
Thom AS, Thony JL, Vauclin M. 1981. On the proper employment of evaporation pans and atmometers in estimating potential transpiration. *Q. J. R. Meteorol. Soc.* **107**: 255–278.
Thomas A. 2000. Spatial and temporal characteristics of potential evapotranspiration trends over China. *Int. J. Climatol.* **20**: 381–396.
Walvoord MA, Plummer MA, Phillips FM, Wolfsberg AV. 2002. Deep arid system hydrodynamics–1. Equilibrium states and response times in thick desert vadose zones. *Water Resour. Res.* **38**(12): 1308.
Walvoord MA, Phillips FM, Stonestrom DA, Evans RD, Hartsough PC, Newman BD, Striegl RG. 2003. A reservoir of nitrate beneath desert soils. *Science* **302**: 1021–1024.
Walvoord MA, Phillips FM. 2004. Identifying areas of basin-floor recharge in the Trans-Pecos region and the link to vegetation. *J. Hydrol.* **292**: 59–74.
Wild M, Gilgen H, Roesch A, Ohmura A, Long CN, Dutton EG, Forgan B, Kallis A, Russak V, Tsvetkov A. 2005. From dimming to brightening: Decadal changes in solar radiation at earth's surface. *Science* **308**: 847–850. DOI: 10.1126/science.1103215.
Wild M, Ohmura A, Makowski A. 2007. Impact of global dimming and brightening on global warming. *Geophys. Res. Lett.* **34**: L04702. DOI: 10.1029/2006GL028031.
Xu C-Y, Lebing G, Jiang T, Chen D, Singh VP. 2006. Analysis of the spatial distribution and temporal trend of reference evaporation and pan evaporation in Changjiang (Yangtze River) catchment. *J. Hydrol.* **327**: 81–93.